HHS Public Access

Author manuscript

Colloids Surf B Biointerfaces. Author manuscript; available in PMC 2018 February 01.

Published in final edited form as:

Colloids Surf B Biointerfaces. 2017 February 01; 150: 261–270. doi:10.1016/j.colsurfb.2016.10.026.

Improving Sensitivity and Specificity of Capturing and Detecting Targeted Cancer Cells with Anti-Biofouling Polymer Coated Magnetic Iron Oxide Nanoparticles

Run Lin[a,b,≠], **Yuancheng Li**[a,≠], **Tobey MacDonald**[c], **Hui Wu**[a], **James Provenzale**[d], **Xingui Peng**[a,e], **Jing Huang**[a], **Liya Wang**[a], **Andrew Y. Wang**[f], **Jianyong Yang**[b], and **Hui Mao**[a,*]

[a]Department of Radiology and Imaging Sciences, Emory University School of Medicine, Atlanta, GA 30322, USA

[b]Department of Radiology, The First Affiliated Hospital of Sun Yat-sen University, Guangzhou, Guangdong 510080, China

[c]Department of Pediatrics, Emory University School of Medicine, Atlanta, GA 30322, USA

[d]Department of Radiology, Duke University Medical Center, Durham, NC 27710, USA

[e]Department of Radiology, The Medical College of Southeastern University, Nanjing, Jiangsu, China

[f]Ocean NanoTech, LLC, San Diego, CA 20046, USA

Abstract

Detecting circulating tumor cells (CTCs) with high sensitivity and specificity is critical to management of metastatic cancers. Although immuno-magnetic technology for *in vitro* detection of CTCs has shown promising potential for clinical applications, the biofouling effect, i.e., non-specific adhesion of biomolecules and non-cancerous cells in complex biological samples to the surface of a device/probe, can reduce the sensitivity and specificity of cell detection. Reported herein is the application of anti-biofouling polyethylene glycol-*block*-allyl glycidyl ether copolymer (PEG-*b*-AGE) coated iron oxide nanoparticles (IONPs) to improve the separation of targeted tumor cells from aqueous phase in an external magnetic field. PEG-*b*-AGE coated IONPs conjugated with transferrin (Tf) exhibited significant anti-biofouling properties against non-specific protein adsorption and off-target cell uptake, thus substantially enhancing the ability to target and separate transferrin receptor (TfR) over-expressed D556 medulloblastoma cells. Tf conjugated PEG-*b*-AGE coated IONPs exhibited a high capture rate of targeted tumor cells (D556 medulloblastoma cell) in cell media (58.7 ± 6.4%) when separating 100 targeted tumor cells from 1×10^5 non-targeted cells and 41 targeted tumor cells from 100 D556 medulloblastoma cells spiked

*Corresponding author. hmao@emory.edu.
≠These authors contributed equally.

into 1 mL blood. It is demonstrated that developed nanoparticle has higher efficiency in capturing targeted cells than widely used micron-sized particles (i.e., Dynabeads®).

Graphical abstract

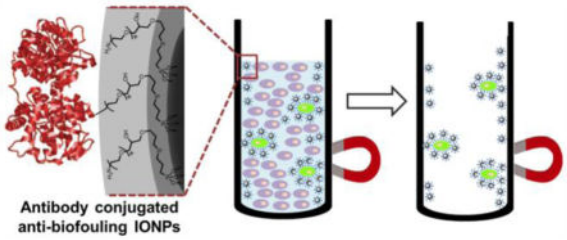

Anti-biofouling PEG-*b*-AGE copolymer coated iron oxide nanoparticles (IONPs) is applied to separate small number of cancer cells in the presence of large excess of non-targeted "background" cells. PEG-*b*-AGE coated IONPs demonstrate improved sensitivity and specificity in targeted cell detection compared with IONPs without anti-biofouling coating and micron-sized Dynabeads® by reducing non-specific cell uptake and protein adsorption.

Keywords

magnetic nanoparticles; cell separation; anti-biofouling; circulating tumor cells; targeting

Introduction

Metastasis accounts for 90% of cancer-related deaths and is a central focus in cancer management.[1–3] Tumor cells can migrate from the primary site through the circulatory systems, (e.g., blood, lymphatic fluid and cerebral spinal fluid) and then spreading to other organs. The presence of circulating tumor cells (CTCs) has been strongly linked to poor prognosis.[4–6] Therefore, timely and accurate survey of the bio-fluid samples to detect rare and an extremely small number of CTCs would greatly improve the early detection of cancer metastasis and clinical decision-making in terms of predicting prognosis as well as stratifying patients for specific and targeted therapeutic strategies. Early studies have shown that the treatment planning based on the information from CTCs may impact the clinical outcomes of the cancer patients with improved survival.[7,8] However, detection of CTCs, particularly in the very early stage of metastasis, is highly challenging due to the inherent difficulty in identifying and capturing an extremely small number of the cancer cells from a typical blood sample volume of 1–7 mL obtained from patients.

Immuno-magnetic separation is the one of the most promising approaches in CTC detection and enumeration, in which magnetic particles are functionalized with ligands to target biomarker molecules over-expressed on tumor cell surfaces, followed by isolation of the particle-tagged cells using an external magnet or magnetic column.[9–18] While conventional immuno-magnetic separation methods with micron-sized magnetic beads, such as Dynabeads®, work well in separating and sorting cells in large number,[19,20] their efficacy in detecting and capturing the extremely small number of CTCs from samples containing a

large excess of other biomolecules or non-targeted cells in the background, e.g., tens of CTCs with millions of other cells in routinely collected blood samples, remains problematic.[9,21,22] Hence, substantial efforts have been made to develop and apply magnetic nanoparticles to immuno-magnetic separation, given the advantages of nanoparticles compared with micron-sized particles, including better suspendability in the sample or media, faster cell surface receptor binding via conjugated targeting ligands, and high affinity of cell binding with more particles bound on each cell and an increased number of cell-nanoparticle interactions and therefore a higher particle-to-/cell ratio.[23–26] More importantly, increasing efforts are focused on maintaining cell integrity and functions for follow-up experiments to interrogate and characterize the captured cells after expanding them in the culture media.[27] Evidently, there is less stress on cells and when cells exposed to nanoparticles comparing to the microparticles, thus preserving cell morphology and functions.[28] In addition to the size effect of magnetic particles, the overall performance of immuno-magnetic separation is also affected by other factors, including the magnetic property of the particles, the strength and gradient of the magnetic field to which the particles are being exposed, the duration and scale of the cell capturing process at a given magnetic field and magnetic particles, the amount of the magnetic particles used and the actual affinity of the functionalized particles to the targeted cells.[29–31] Among these, the surface modification and fabrication of magnetic nanoparticles to alter or reduce the biofouling effect are of particular interest. The biofouling effect, i.e. non-specific adsorption of macromolecules, such as proteins, from the biological fluid samples onto the surface of the nanoparticles, may compromise the affinity of the targeting particles to the cells, as the surface properties and functions of particles may be altered after protein adsorption.[32–35] Furthermore, the non-specific off-target cell binding and uptake of nanoparticles by non-target cells make differentiating CTCs from normal cells difficult.[36–39] Therefore, an approach to eliminate or reduce the non-specific interactions between nanoparticles and the unwanted materials and cells is highly desirable for applying immuno-magnetic separation techniques to CTC detection.

Herein, we report the development of ligand-functionalized anti-biofouling polyethylene glycol-*block*-allyl glycidyl ether (PEG-*b*-AGE) polymer coated magnetic iron oxide nanoparticles (IONPs) for improved targeting and capturing small numbers of tumor cells in the presence of a large excess of non-target cells. The advantages and the efficiency of cell capture using anti-biofouling PEG-*b*-AGE coated magnetic IONPs in cell separation were investigated by comparing with micron-sized magnetic beads. When coupled with transferrin (Tf) as a targeting moiety, PEG-*b*-AGE coated IONPs enabled binding and separating cells with a high level of transferrin receptor (TfR) expression. The efficiency of targeting and capturing TfR over-expressed cancer cells with developed IONPs was tested using medulloblastoma cells that are known to metastasize through cerebral spinal fluid.[40] With anti-biofouling properties, our IONPs have shown improved capability in capturing targeted cancer cells with high sensitivity and specificity by significantly reducing the “background” from the non-specific capture of unwanted cells.

Materials and Methods

Materials

Holo-transferrin (Tf, ≥97%), fluorescein isothiocyanate (FITC), tetramethylrhodamine (TRITC) and poly-L-lysine (PLL, MW 70,000–150,000) were purchased from Sigma-Aldrich. CellTracker™ Green 5-chloromethylfluorescein diacetate (CMFDA), ProLong Gold anti-fade mountant with 4′, 6-diamidino-2-phenylindole (DAPI), Vybrant Dil cell-labeling solution and magnetic beads with 4.5 μm in diameter (Dynabeads® M-450 Epoxy) were purchased from Life Technologies. Sulfosuccinimidyl 4-(N-maleimidomethyl)cyclohexane-1-carboxylate (sulfo-SMCC), 2-iminothiolane (Traut's reagent), N-hydroxysulfosuccinimide (sulfo-NHS), 1-ethyl-3-(3-dimethylaminopropyl)carbodiimide hydrochloride (EDC), bicinchoninic acid (BCA) protein assay kit, fetal bovine serum (FBS), streptomycin and penicillin (10,000 U/mL penicillin, 10,000 μg/mL streptomycin in 0.85% saline) were purchased from Thermo Fisher Scientific. Eagle's Minimum Essential Medium (EMEM), Dulbecco's Modification of Eagle's Medium (DMEM), Roswell Park Memorial Institute 1640 (RPMI 1640) medium and phosphate-buffered saline (PBS) were purchased from Corning. Carboxylate-functionalized, water soluble IONPs with 20 nm core size (SHP20) were obtained from Ocean NanoTech LLC. EasySep Magnet and 40% paraformaldehyde were purchased from StemCell Technologies (Catalog number 18000) and Electron Microscopy Sciences, respectively. The whole blood used in this study was collected from an adult landrace cross pig. Blood was then placed in blood collection tubes (BD Vacutainer® lithium heparin 158 usp). The blood was used within 12 hours after collection.

Preparation and characterization of PEG-b-AGE coated IONPs

IONPs made from thermo-decomposition and coated with oleic acids are water insoluble, and therefore, need to be stabilized in aqueous media via a ligand exchange reaction to replace oleic acids with hydrophilic molecules, such as PEG-*b*-AGE copolymer. The procedures of synthesis of PEG-*b*-AGE copolymer and coating IONPs with anti-biofouling PEG-*b*-AGE copolymer were adapted from the protocol previously reported by our group.[41] The core sizes of the IONPs before and after coating and surface functionalization were measured using transmission electron microscopy (TEM, H-7500, Hitachi). The hydrodynamic sizes and surface charges of coated IONPs were assessed using a dynamic light scattering (DLS) instrument (Zetasizer Nano S90, Malvern). The averaged hydrodynamic size and zeta potential values were calculated from three measurements for each sample using number-weighted statistics. Iron concentrations were determined by colorimetric spectroscopy as described in literature.[42]

Conjugation of transferrin

Amino group-bearing PEG-*b*-AGE coated IONPs were conjugated with Tf or FITC pre-labeled Tf (FITC-Tf) through a two-step conjugation procedure using the heterobifunctional crosslinker sulfo-SMCC. For the control, Tf or FITC-Tf was conjugated to magnetic IONPs SHP20 via cross-linking of carboxyl groups to the amino groups on the side chain of Tf or FITC-Tf noting that SHP20 has the same hydrophobic IONP cores as those used for PEG-*b*-AGE coating. Micron-sized magnetic beads (Dynabeads®, 4.5 μm in diameter) were also

prepared for comparison experiments. In this case, Tf or FITC-Tf was conjugated to the Dynabeads following the manufacturer's instructions (Supplementary Information).

Specificity of cell binding by Tf-conjugated nanoparticles

Medulloblastoma D556 cells with over-expressed TfR, lung cancer A549 cells with very low TfR expression and mouse macrophage Raw264.7 cells were cultured in EMEM, DMEM and RPMI1640, respectively. Media was supplemented with 10% (v/v) FBS, 1% (v/v) streptomycin and penicillin and cells were grown in a 5% CO_2 atmosphere at 37 °C. 2×10^4 cells were seeded into 8-well chamber slides (Lab-Tek II, Thomas Scientific) and grown for 24 hours before experiments were performed. Culture media was aspirated and replaced by particle-containing media and the cells were cultured for three hours at 37 °C followed by Prussian blue staining to verify the uptake of IONPs. To validate the effect of PEG-*b*-AGE coated IONPs on reducing non-specific cellular uptake, PEG-*b*-AGE coated IONPs or SHP were incubated with Raw264.7 macrophage cells with iron concentrations of 0.2 or 0.025 mg/mL, respectively. Tf conjugated PEG-*b*-AGE coated IONPs (Tf-IONP) or SHP (Tf-SHP) at the Fe concentration of 0.2 mg/mL were also used to treat D556 or A549 cells to examine the specific binding and internalization of Tf-conjugated particles with non-targeted PEG-*b*-AGE coated IONPs or SHP as a control. Binding specificity was further tested and confirmed with a blocking assay by incubating D556 medulloblastoma cells with 400 molar excess of Tf for 30 minutes to block TfR prior to the addition of FITC-Tf- IONPs or FITC-Tf-SHP.

Influence of protein adsorption on receptor targeting

To examine the effect of non-specific protein adsorption on the particle surface which interferences targeting of nanoparticles and the anti-biofouling properties, FITC-Tf-IONP and FITC-Tf-SHP (Fe concentration of 1 mg/mL) were pre-treated with 50% (v/v) FBS in PBS at room temperature for one hour incubation. The FBS treated nanoparticles were separated magnetically from the solution by applying an external magnet for two hours, followed by re-suspending the collected materials in PBS. The separation-resuspension was repeated three times. The protein concentration was determined using the BCA protein assay as described in literature.[41] The protein corona concentration was defined by the difference in protein concentrations (μg protein/mg IONP) between FBS treated and non-treated IONPs. Both FBS pre-treated and non-treated FITC-Tf-IONP and FITC-Tf-SHP were then incubated with D556 medulloblastoma and A549 lung cancer cells in culture media with an iron concentration of 0.2 mg/mL at 37 °C for three hours. Afterwards the supernatant was removed, and the cells were rinsed with PBS three times. For fluorescence imaging, 2×10^4 cells (either D556 medulloblastoma or A549 lung cancer cells) were seeded into an 8-well chamber slide and grown for 24 hours before incubating with nanoparticles. After incubation, cells were fixed with 4% paraformaldehyde for 20 minutes, followed by rinsing cells three times with deionized water. The slide was then mounted with gold anti-fade mounting reagent containing DAPI. To evaluate the effect of the protein corona on cell targeting, fluorescence signals of FITC from the FBS pre-treated and non-treated nanoparticles taken up by cells were measured. 5×10^3 D556 medulloblastoma or A549 lung cancer cells were seeded into a 96-well plate. The cells were grown at 37 °C for 24 hours before incubating with nanoparticles. Afterwards, cells were lysed for the measurement of

fluorescence signal from FITC on a plate reader to assess whether the protein adsorption on the IONP surface might affect IONPs binding to the cells. The fluorescence signal intensity was averaged from six wells.

Sensitivity of cell capture

To validate whether nanoparticles are more sensitive than micron-sized particles in cell separation, the efficiencies of capturing TfR over-expressed D556 medulloblastoma cells using PEG-*b*-AGE coated IONP and Dynabeads® both conjugated with Tf were evaluated. 2×10^4 medulloblastoma D556 cells were stained with Dil (red fluorescence) according to the manufacturer's manual, and then seeded into a 12-well plate and cultured for two days. Cells were then incubated either with FITC-Tf-IONPs at the iron concentration of 0.2 mg/mL or 2×10^6 Tf-Beads in 1 mL of PBS for two hours at 37 °C. Afterwards, cells were washed with PBS three times, detached from the plate, and transferred into a tube for magnetic separation. An external magnet was applied to the tube for 45 minutes at room temperature to allow D556 cells bound with the magnetic particle to attach to the tube. The supernatant was separated from the attached cells, which were then re-suspended with PBS. Both supernatant and cell resuspension were transferred to PLL-coated chambers and cultured for two hours at 37 °C for the cells to attach to the chamber. The collected cells were then fixed with 4% paraformaldehyde for 20 minutes before DAPI staining for nucleus. The average number of beads bound to the cells was calculated based on measuring 20 cells randomly selected from the microscopic field of view. The cell capture efficiency was defined by Equation 1,

$$\text{Capture efficiency} = N_{capture}/(N_{capture}+N_{super}) \quad \text{Eq. 1}$$

where $N_{capture}$ and N_{super} are the average numbers of cells counted from six different microscopic views (10X magnification) of magnetically captured cells and the cells in supernatant respectively.

Specificity of cell capture

To investigate the effect of the anti-biofouling coating on the specificity of capturing targeted cells, Tf-IONPs or Tf-SHP were cultured with a mixture of 1×10^5 TfR over-expressed D556 cells pre-stained with CMFDA (green fluorescence) and 1×10^5 A549 cells with low expression level of TfR as "background" in a final volume of 1.0 mL and iron concentration of 0.2 mg/mL. After incubating at 37 °C for two hours and separating magnetically for 45 minutes, the supernatant was removed (Scheme 1). The captured cells were re-suspended in PBS and examined by flow cytometry (FCM, BD FACSCanto II RUO Special Order System, BD Biosciences) or smeared onto a slide and fixed with 4% paraformaldehyde in PBS, followed by DAPI (blue fluorescence) staining for fluorescent microscopy (BX41, Olympus). The cell separation specificity was defined by Equation 2,

$$\text{Separation specificity} = N_{D556}/(N_{D556}+N_{A549}) \quad \text{Eq. 2}$$

where N_{D556} and N_{A549} are the average numbers of D556 medulloblastoma cells (showing both green and blue fluorescence) and A549 lung cancer cells (showing only blue fluorescence) counted from three different microscopic views (10X magnification) of the captured cells.

To further examine the specificity of isolating targeted cells using anti-biofouling magnetic IONPs, the separation of target cells in the presence of an excess amount of un-wanted cells was investigated using FITC-Tf-IONP with the anti-biofouling polymer coating and FITC-Tf-SHP with the conventional polymer coating. Briefly, 100 CMFDA pre-stained D556 medulloblastoma cells with over-expressed TfR were spiked into the culture medium containing 1×10^5 A549 lung cancer cells that have very low level of TfR expression. FITC-Tf-IONPs or FITC-Tf-SHP were added to the cell mixture at the final volume of 1.0 mL and iron concentration of 0.2 mg/mL. The solutions were cultured at 37 °C for two hours before being put in an external magnet for 45 minutes at room temperature to allow the cells bound to the IONPs to form a pellet under magnetic force. The supernatant was removed and the captured cells were re-suspended with PBS, transferred to PLL-coated chamber and cultured at 37 °C for two hours allowing the cells to attach to the chamber. The cells were washed three times with PBS and then fixed with 4% paraformaldehyde in PBS for 20 minutes before nuclear staining with DAPI. Fluorescence imaging of the green fluorescence from FITC labeled IONPs and blue fluorescence from DAPI stained nuclei was used to identify target D556 medulloblastoma cells (green from FITC labeled IONPs and blue from DAPI) or non-target A549 lung cancer cells (only blue from DAPI).

Targeted cell separation from the blood

To further test whether anti-biofouling IONPs can maintain high efficiency and specificity in separating targeted rare cells in more a sparse, clinically relevant blood sample, FITC-Tf-IONP was incubated with 100 D556 medulloblastoma cells spiked into 1 mL of whole porcine blood at 37 °C in a 2-mL Eppendorf centrifuge tube with an iron concentration of 0.2 mg/mL. The tube was rotated continuously for three hours. Afterwards, the tube was placed in an EasySep magnet for 45 minutes to allow the IONPs with captured cells to attach to the wall. The blood was then carefully removed, leaving behind the magnetic cell pellet. The captured cells were re-suspended in DMEM, and then transferred to PLL-coated chamber. The cells were cultured at 37 °C for two hours to attach to the chamber. The cells were washed three times with PBS and then incubated with TRITC-Tf with a Tf concentration of 0.1 mg/mL at 37 °C for 30 minutes. The D556 medulloblastoma cells tagged with fluorescent TRITC-Tf then were distinguished from other eukaryotic cells. The cells were washed three times with PBS and then fixed with 4% paraformaldehyde in PBS for 20 minutes before DAPI staining. The number of captured D556 medulloblastoma cells was counted microscopically.

Proliferation of cells captured from the blood

To test if the magnetic Tf-IONP captured D556 medulloblastoma cells remain viable and can proliferate, cells isolated from whole blood were re-suspended in the culture medium, and then transferred to PLL-coated chamber followed by culture at 37 °C for 72 hours. After washing thrice with PBS, the cells were then incubated with TRITC-Tf (0.2 mg Tf/mL medium) at 37 °C for 30 minutes. Following the incubation with TRITC-Tf, the cells were washed with PBS again for three times. 4%paraformaldehyde in PBS was used to fix the cells for 20 minutes. Cell nuclei were stained with DAPI for cell counting. Number of D556 medulloblastoma cells after proliferation was counted microscopically to evaluation the viability of captured cells. Only cells with both DAPI and TRITC fluorescent signals were counted as D556 cells. 50 D556 medulloblastoma cells were proliferated for 72 hours as the control. By assuming 41 D556 medulloblastoma cells were captured for proliferation, the viability of captured cells was defined by Equation 3,

$$\text{Viability of captured cell} = 50 \times N_{cap}/N_{control}/41 \quad \text{Eq. 3}$$

where N_{cap} is the number of proliferated captured D556 medulloblastoma cells and $N_{control}$ is the number of proliferated D556 medulloblastoma cells in the control.

Statistical analysis

The sensitivity and specificity of cell capture using magnetic particles were calculated and the results were presented as the mean ± standard deviation. The rates of cell recovery from the mixture containing the same number of D556 medulloblastoma cells and A549 lung cancer cells using different forms of magnetic particles were calculated and compared. A two-tailed unpaired *t* test was used to determine whether the results were significant. The level of significance was set at $P < 0.05$.

RESULTS

Characterization of nanoparticles and micron-sized beads with different surface properties

The PEG-*b*-AGE coating polymer was synthesized and used to coat magnetic IONPs as described in the previous work by Li et al.[41] Polymer coated IONPs (with the core size of 20 nm) were mono-dispersed in the aqueous solution with a hydrodynamic diameter of ~30 nm and zeta potential of +15.57 mV as shown in TEM images (Figure 1A) and DLS data (Figure 1B and Table 1). The PEG-*b*-AGE amphiphilic polymer not only allows for transferring hydrophobic oleic acid coated IONPs from organic solvent to water, but also stabilizes the coated IONPs resulting in the mono-dispersion of nanoparticles with a narrow distribution of hydrodynamic sizes for further applications in aqueous solutions.

Tf was conjugated with magnetic IONPs as the ligand for targeting TfR over-expressed cells. The successful conjugation of Tf onto PEG-*b*-AGE coated IONPs or SHP was confirmed by the increased hydrodynamic sizes and shifted zeta potentials as shown in Table 1. Conjugation of Tf and FITC-Tf with micron-sized Dynabeads® was also carried out. (Supplementary Information).

Consistent with our previous report on anti-biofouling properties of PEG-*b*-AGE coated IONPs with 10 nm core size, the 20 nm core size PEG-*b*-AGE coated IONPs prepared in this work exhibited no uptake of non-targeted PEG-*b*-AGE coated IONPs by either D556 or A549 cells. In comparison, we observed uptake of targeted Tf-IONPs by D556 cells with TfR over expression but not by A549 cells which did not have over expression of the TfR (Supplementary Information S2). On the contrary, when D556 or A549 cells were treated with SHP (IONP without anti-biofouling coating) or Tf-SHP, great amounts of IONP uptake were observed in both cell lines. The specific uptake of Tf-IONPs by D556 cells was further verified by the blocking experiments with excess amount of Tf binding to TfR to block the targets prior to the addition of Tf-IONPs. As expected, significantly reduced uptake of nanoparticle by the cells treated with free Tf was observed (Supplementary Information, Figure S3). When incubated with macrophage cells, PEG-*b*-AGE coated IONPs exhibited no macrophage uptake while Tf conjugated Tf-IONPs showed only moderate uptake of by macrophages due to the low expression level of TfR on macrophages (Supplementary Information S2).[43]

Effect of anti-biofouling coating on the protein adsorption and biomarker targeting

Since the presence of a protein corona has been shown to affect the biomarker targeting of ligand-conjugated nanomaterials,[32,33] we further assessed the targeting capability of PEG-*b*-AGE polymer coated IONPs in the targeted immuno-magnetic separation after exposing the particles to serum proteins. The incubation of FITC-Tf-SHP with FBS (50% in PBS, ~ 20 mg protein/mL) resulted in the protein adsorption on FITC-Tf-SHP at the protein concentration of 346 μg/mg Fe. As a comparison, the concentration of protein adsorbed onto the anti-biofouling PEG-*b*-AGE polymer coated FITC-Tf-IONPs was found to be 16 μg/mg Fe (Supplementary Information Figure S4). After FBS pre-treated or non-treated FITC-Tf-IONP or FITC-Tf-SHP were incubated with D556 medulloblastoma or A549 lung cancer cells at 37 °C for three hours, fluorescence imaging was used to determine the amount of FITC labeled Tf-IONPs bound to cells. As shown in Figure 2, D556 medulloblastoma cells did not exhibit an obvious difference in taking up FITC-Tf-IONPs and FBS pre-treated FITC-Tf-IONPs (Figure 2A and B) However, FITC-Tf-SHP exhibited decreased cellular uptake by D556 medulloblastoma cells after the nanoparticle was treated with FBS (Figure 2C and D). These results indicated that anti-biofouling FITC-Tf-IONP maintained cell targeting by preventing the adsorption of proteins from medium, while protein absorption attenuated the targeting capability of FITC-Tf-SHP. No IONP uptake by A549 lung cancer cells was observed for either FBS treated or non-treated FITC-Tf-IONPs (Figure 2E and F), and little difference in FITC-Tf-SHP uptake level was observed for A549 lung cancer cells (Figure 2G and H) after FITC-Tf-SHP was treated with FBS.

When using the fluorescence signal intensity to estimate the level of FITC labeled targeting IONPs (FITC-Tf-IONP or FITC-Tf-SHP) bound to D556 cells under the interference of protein adsorption, we observed a 53% signal intensity drop after FITC-Tf-SHP was pre-treated with FBS. In contrast, only a 2% signal intensity change was observed from the FITC-Tf-IONP after pre-treatment with FBS (Figure 2I). In addition, the signal intensity ratio of A549 cells (non-targeted)/D556 cells (targeted) increased from 50% (FBS non-treated) to 67% (FBS pre-treated), indicating more non-targeted A549 cells being captured

by the FITC-Tf-SHP as it became less capable of differentiating targeted cells and non-targeted cells after the exposure to proteins in medium. As a comparison, the ratio of the signal intensity of A549 cells (non-targeted)/D556 cells (targeted) increased from 13% (FBS non-treated) to 20% (FBS pre-treated) for FITC-Tf-IONP, suggesting the limited influence of proteins to the specificity of cell targeting. Although the cellular uptake levels of nanomaterials may also depend on other properties of coating materials and surface,[32] the difference in particle uptake using FBS pre-treated or non-treated magnetic IONPs is likely indicative of the interference of the protein corona on the surface of nanoparticles with receptor targeting.

Sensitivity of cell capture with magnetic nanoparticles

To assess the sensitivity of cell capture, we estimated the number of cells captured and separated by an external magnet after FITC-Tf-IONP or Dynabeads® conjugated with FITC-Tf (FITC-Tf-Beads) were incubated with 2×10^4 D556 medulloblastoma cells for two hours at 37 °C, respectively. Counting the number of cells observed based on strong fluorescence from FITC and DAPI (Figure 3A to C), 95.5 ± 1.4% of the D556 medulloblastoma cells were captured by FITC-Tf-IONP and weak fluorescence from FITC was observed for the cells left in the supernatant (Figure 3D to F), indicating sufficient magnetism from nanoparticles for magnetic separation. In comparison, only 21.3 ± 1.7% of D556 cells could be captured using FITC-Tf-beads (Figure 3G) using the experimental conditions of this study, compared with 95.5% using FITC-Tf-IONPs.

As shown in Figure 4, for the cells treated with FITC-Tf-bead, only 5.45 ± 3.19 (n = 20) beads can attach onto each captured cell even when the initial ratio of beads to cell was 100: 1 (Figure 4A to E). In contrast, a large number of Tf-IONPs could be targeted and bound to a single cell indicated by the increased green fluorescence from the FITC (Figure 4F to H), thus providing improved capability for magnetic isolation. The D556 cells separated by Tf-IONP were further examined by TEM to validate the large number of IONP accumulation inside the cells (Supplementary Information, Figure S5).

Specificity of receptor mediated cell capture and separation

While many strategies have been developed for improving the sensitivity of CTC detection, achieving higher sensitivity is often accompanied with losing specificity (i.e. capturing targeted cells but not unwanted cells). To test whether applying anti-biofouling coating strategy may improve the specificity of isolating targeted cells, we used Tf-IONPs to capture targeted cells from a mixture containing an equal number (1×10^5) of non-target cells. Tf-SHP was used for comparison. From a mixture containing an equal number of D556 medulloblastoma cells (pre-stained by CMFDA) and A549 lung cancer cells, Tf-IONP successfully captured 79.0 ± 4.0% (n = 3) of targeted D556 medulloblastoma cells but only 16.7 ± 4.4% (n = 3) of off-target A549 lung cancer cells. The specificity of targeted cell capture by the Tf-IONPs was found to be 83%. Meanwhile, Tf-SHP also captured 87.1 ± 5.2% (n = 3) of the D556 medulloblastoma cells from the cell mixture. However, 79.3 ± 4.2% (n = 3) of non-targeted A549 lung cancer cells were also captured by Tf-SHP, resulting in a specificity of 53% (Figure 5A). Cells separated by Tf-IONP contained fewer non-targeted A549 lung cancer cells (Figure 5B to D) than those captured by Tf-SHP

(Figure 5E to G). The flow cytometry evaluation of the captured cells was in great agreement with the cell enumeration. The similar signal intensity from D556 medulloblastoma cells (peaks centered at 10^4) separated by Tf-IONP and Tf-SHP, as well as the much lower signal from A549 lung cancer cells (peaks centered at 10^3) captured by Tf-IONP than Tf-SHP, support that the higher proportion of targeted cells (D556 cells with green fluorescence from CMFDA) among all captured ones isolated using Tf-IONP (Figure 5H and I).

To further evaluate the potential of PEG-*b*-AGE coated IONP in rare CTCs detection, the separation of 100 CMFDA pre-stained D556 cells from 1×10^5 A549 cells using Tf-IONP was investigated with Tf-SHP as control. It was found that 58.7 ± 6.4% (n=3) and 62.7 ± 7.6 % (n=3) of targeted D556 medulloblastoma cells were separated using both Tf-IONP and Tf-SHP respectively (Figure 6G) with no statistically significant difference ($p>0.05$), suggesting that both Tf-IONP and Tf-SHP (with the same size of core and magnetic properties) possessed similarly high sensitivity in isolating cells as low as 100 cells/mL. However, cells captured by Tf-SHP contained a great amount of non-targeted A549 lung cancer cells (Figure 6D to F), leading to a lower specificity rate, while Tf-IONP mainly captured D556 medulloblastoma cells (Figure 6A to C).

Capturing targeted cancer cells from the whole blood and viability of captured cells

Blood samples with CTCs also contains a variety of materials such asa multitude of other cells and macromolecules including various normal cells, proteins, peptides, and other biomolecules which may cause non-specifically interactions and even adsorption on the nanoparticle surface, interfering cell targeting by the nanoparticles. To examine the potential of using developed anti-biofouling IONPs in capturing CTCs in blood, we spiked whole blood samples with cancer cells to mimic clinical samples acquired from cancer patients. FITC-Tf-IONPs were used to capture 100 D556 medulloblastoma cells that were spiked into 1 mL of whole blood collected from the pig following the procedure described in **Materials and Methods** section. We observed that 41 out of 100 D556 cells were successfully isolated from the blood sample using the FITC-Tf-IONPs. Along with the targeted cancer cells, a few red blood cells were also captured (Figure 7A). Considering that 1 mL of blood contains several millions of red blood cells,[44] the result supports the potential of the reported immuno-magnetic cell capture system for isolating CTCs in patient samples. As many normal and diseased cells, including red blood cells, also express low levels of TfR on cell membrane,[45] it is worth noting that non-cancerous cells in the blood with TfR expression might also be captured using FITC-Tf-IONPs, resulting in an off-target “background”. Although a number of red blood cells were also isolated (Figure 7A), there is no detectable signal of FITC or TRITC from the captured red blood cells (Figure 7B, D). The results suggest that under our experimental conditions, the binding and uptake of FITC-Tf-IONPs by red blood cells is minimal compared to that by D556 medulloblastoma cells with over-expressed TfR. Accounting for the total all observed fluorescent signals (DAPI, FITC, and TRITC) into consideration, we suggest it can be concluded that targeted D556 cells were captured from the blood with little eukaryotic cells present, as the DAPI staining only shows one nucleus which perfectly overlaid with the FITC (FITC-Tf-IONP) and TRITC (TRITC-Tf) signal (Figure 7B to E).

Since the captured cancer cells are often used in further molecular or genetic characterizations[46,47] for diagnosis or investigation, the number of cells captured as well as the integrity and viability of captured cells are important. We investigated the viability of the captured cells using a cell proliferation assay. Captured cells were proliferated for 72 hours with 50 non-treated D556 medulloblastoma cells proliferated as a control. After proliferation, TfR over-expressed D556 cells were labeled with TRITC by incubation with TRITC-Tf. We observed that the captured D556 cells maintain the ability to proliferate (Figure 8B–D). The number of D556 cells proliferated from the captured cells was 194 compared to 231 from the non-treated control after counting the cells microscopically (Figure 8). By assuming that 41 D556 cells were separated from blood for proliferation, the viability of captured D556 medulloblastoma cells was determined to be 89%.

DISCUSSION

Since the early detection of cancer metastasis requires capturing a very small number of CTCs in bio-fluid samples, such as blood, cerebral spinal fluid or urine, magnetic particles and probes capable of highly specific biomarker targeting are crucial for CTC detection and separation. These biological samples typically contain a high level of proteins, other charged macromolecules and many types of non-CTC cells.[48] The biofouling caused by non-specific macromolecule and protein adsorption on the surface of functionalized nanoparticles or devices has been recognized as one of the major hindrances in biomarker-targeted applications of nanomaterials and technology.[49,50] In addition, mononuclear phagocytes, such as macrophage cells, are abundant in these samples.[51] Since macrophages are known to engulf exogenous particles, reducing the off-target cellular uptake of magnetic particles may also lead to better specificity and sensitivity for detection of CTCs. Using PEG-*b*-AGE polymer coating, anti-biofouling Tf-IONP reported in this work exhibited much less protein adsorption (16 μg/mg Fe) on the surface compared with Tf-SHP (346 μg/mg Fe). Since the presence of a protein corona has been shown to affect the biomarker targeting of ligand-conjugated nanomaterials,[32,33] the anti-biofouling Tf-IONP was able to maintain the targeting capability in protein containing media by reducing the surface protein adsorption which were demonstrated in the cell targeting experiments (Figure 2). In cell uptake experiments, PEG-*b*-AGE coated IONPs exhibited strong anti-biofouling effect by showing no cellular uptake by D556 medulloblastoma, A549 lung cancer, or Raw264.7 macrophage cells. Minimal Raw264.7 macrophage uptake of Tf-IONP may be attributed to a very low level of TfR expression in the Raw264.7 cells.

The reported anti-biofouling properties of Tf-IONP also demonstrated higher specificity in capturing targeted cells in the presence of a large number of unwanted cells in both culture media and the blood samples we prepared to mimic patient samples. When tested with a cell mixture of 100 targeted D556 cells spiked in 1×10^5 unwanted A549 cells, the anti-biofouling Tf-IONP was able to capture 79.0 ± 4.0% of the targeted D556 medulloblastoma cells with only 16.7 ± 4.4% off-targeted A549 lung cancer cells. The specificity of targeted cell capture by Tf-IONP was found to be 83%. In comparison, specificity of Tf-SHP without additional anti-biofouling modification was only 53% in the same experiment, even though both Tf-IONP and Tf-SHP possessed similarly high sensitivity (58.7 ± 6.4% *vs.* 62.7 ± 7.6 %). In more clinically relevant blood samples, one mL of blood contains 4 to 6 million

red blood cells, 4,000 to 11,000 white blood cells, and 200,000 to 500,000 platelets.[44] To obtain reliable detection, the ratio of captured targeted cells to non-targeted cells is believed to be 1:10 to 1:100 following cell separation.[31] In our experiments with blood sample spiked with cancer cells, by counting the number of D556 medulloblastoma cells and other non-targeted cells in four randomly picked microscopic views (40X) after all captured cells were fixed and stained, the ratio of targeted cells (D556) to non-targeted cells (all other cells) was found to be 1:81 ± 9, which fell into the feasible range (Figure 7A). The emphasis of pushing sensitivity of CTC detection without compromising specificity is important as inadequate specificity not only contributes to making the process of cell separation labor-intensive and time-consuming, but it also, in turn, leads to a high false-positive rate owing to the low signal-to-noise ratio. For instance, early reports indicated that separation of CTCs by the CellSearch® technology, the only FDA-approved CTC detection product available commercially, yields only 0.01–0.1% in purity (CTCs/captured cells).[52,53]

It is also worth noting that currently most immuno-magnetic separation procedures are performed using commercially available micron-sized magnetic particles or beads. The major advantage of using micron-sized beads is their strong magnetism, thus rendering them to be easily separated using very low-field bench-top permanent magnets. This process is robust and efficient when extracting large numbers of wanted cells from a small amount of unwanted cells. However, for the separation of a small number of targeted cells (as in most clinical settings), nanoparticles may have significant advantages over using micron-sized particles or beads[2], including (1) more surface area for conjugating targeting ligands, thus increasing the probability of nanoparticles interactions with cell surface markers; (2) increased numbers of nanoparticles bound or even internalized by the targeted cells than micron-sized beads, thus collectively, to gain sufficient magnetism for magnetic separation, and (3) maintenance of cell integrity and viability with less magnetic force-induced stress on the captured cells when additional molecular characterizations of the captured cells need to be carried out, which typically involve in culture and expanding a few or even single captured cells. The results of this study further support the as PEG-*b*-AGE coated FITC-Tf-IONPs were found to be much more sensitive in capturing D556 cells than FITC-Tf-beads prepared from the Dynabeads® ((95.5 ± 1.4% *vs.* 21.3 ± 1.7%). The low capture sensitivity of micron-sized beads can be explained by the higher steric hindrance and less ligand-to-cell interactions, given that Dynabeads® and cells are of the same order of magnitude in size. The larger the bead, the harder it binds to cells through ligand-to-target interactions.

Conclusion

We have demonstrated that, by applying the anti-biofouling PEG-*b*-AGE polymer coating to IONPs, improved sensitivity and specificity were achieved in biomarker-directed cell capture and separation with magnetic iron oxide nanoparticles. A very small number of spiked cancer cells can also be separated from whole blood in a biologically-relevant ratio of targeted to non-targeted cells, while the captured cancer cells maintained viability to proliferate. The excellent performance of this system is likely due to the significantly reduced protein corona formation on the surface of nanoparticles as a result of the anti-biofouling polymer coating and off-target capture of “background” non-specific cells. Furthermore, magnetic nanoparticles functionalized with targeting ligands exhibited higher

efficiency in targeted cell capture and separation than micron-sized magnetic bead in both sensitivity and specificity. With anti-biofouling properties, developed IONPs may offer ameliorated capability for capturing targeted cells, such as circulating cancer cells, in bio-fluid samples with high sensitivity and specificity.

Supplementary Material

Refer to Web version on PubMed Central for supplementary material.

Acknowledgments

This work is supported in parts by NIH R01CA154846-02 (HM and LY), NCI's Cancer Nanotechnology Platform Project (CNPP) grant U01CA151810-02 (HM and LY), a seed grant from the Center for Pediatric Nanomedicine of Children's Healthcare of Atlanta (HM and TM), and Oversea Study Program of Guangzhou Elite Project (GEP, 11YB18) (RL). YL and RL contributed equally to this work. The authors thank Dr. Candace C. Fleischer for her careful reviewing and proofreading of the manuscript. The swine blood sample was generously provided by the laboratory of Dr. Franklin West in the Department of Animal Sciences, University of Georgia.

References

1. Hanahan D, Weinberg RA. Cell. 2000; 100:57. [PubMed: 10647931]
2. Pantel K, Alix-Panabières C, Riethdorf S. Nature Reviews Clinical Oncology. 2009; 6:339.
3. Valastyan S, Weinberg RA. Cell. 2011; 147:275. [PubMed: 22000009]
4. Goldkorn A, Ely B, Quinn DI, Tangen CM, Fink LM, Xu T, Twardowski P, Van Veldhuizen PJ, Agarwal N, Carducci MA. Journal of Clinical Oncology. 2014; 32:1136. [PubMed: 24616308]
5. Sosa MS, Bragado P, Aguirre-Ghiso JA. Nature Reviews Cancer. 2014; 19:611.
6. Rack B, Schindlbeck C, Jückstock J, Andergassen U, Hepp P, Zwingers T, Friedl TW, Lorenz R, Tesch H, Fasching PA. Journal of the National Cancer Institute. 2014; 106:dju066. [PubMed: 24832787]
7. Zieglschmid V, Hollmann C, Böcher O. Critical Reviews in Clinical Laboratory Sciences. 2005; 42:155. [PubMed: 15941083]
8. Smerage JB, Barlow WE, Hortobagyi GN, Winer EP, Leyland-Jones B, Srkalovic G, Tejwani S, Schott AF, O'Rourke MA, Lew DL. Journal of Clinical Oncology. 2014; 32:3483. [PubMed: 24888818]
9. Yoon HJ, Kozminsky M, Nagrath S. ACS nano. 2014; 8:1995. [PubMed: 24601556]
10. Onstenk W, Kraan J, Mostert B, Timmermans MM, Charehbili A, Smit VTHBM, Kroep JR, Nortier JWR, Ven Svd, Heijns JB, Kessels LW, van Laarhoven HWM, Bos MMEM, van de Velde CJH, Gratama J-W, Sieuwerts AM, Martens JWM, Foekens JA, Sleijfer S. Molecular Cancer Therapeutics. 2015; 14:821. [PubMed: 25552367]
11. Kim TH, Yoon HJ, Stella P, Nagrah S. Biomicrofluidics. 2014; 8:064117. [PubMed: 25553193]
12. Murlidhar V, Zeinali M, Grabauskiene S, Ghannad-Rezaie M, Wicha MS, Simeone DM, Ramnath N, Reddy RM, Nagrah S. Small. 2014; 10:4895. [PubMed: 25074448]
13. Scarberry KE, Dickerson EB, McDonald JF, Zhang ZJ. Journal of the American Chemical Society. 2008; 130:10258. [PubMed: 18611005]
14. Huang Y-Y, Chen P, Wu C-H, Hoshino K, Sokolov K, Lane N, Liu H, Huebschman M, Frenkel EP, Zhang JXJ. Scientific Reports. 2015; 5:16047. [PubMed: 26538094]
15. Huang Y-Y, Hoshino K, Chen P, Wu C-H, Lane N, Huebschman M, Liu H, Sokolov K, Uhr JW, Frenkel EP, Zhang X. Biomedical Microdevices. 2013; 15:673. [PubMed: 23109037]
16. Chen P, Huang Y-Y, Hoshino K, Zhang JXJ. Scientific Reports. 2015; 5:8745. [PubMed: 25735563]
17. Chen P, Huang Y-Y, Hoshino K, Zhang X. Lab on a Chip. 2014; 14:446. [PubMed: 24292816]
18. Chen J-Y, Tsai W-S, Shao H-J, Wu J-C, Lai J-M, Lu S-H, Hung T-F, Yang C-T, Wu L-S, Chen J-S, Lee W-H, Chang Y-C. PLoS One. 2016; 11:e0149633. [PubMed: 26938471]

19. Longo PG, Laurenti L, Gobessi S, Sica S, Leone G, Efremov DG. Blood. 2008; 111:846. [PubMed: 17928528]
20. Petlickovski A, Laurenti L, Li X, Marietti S, Chiusolo P, Sica S, Leone G, Efremov DG. Blood. 2005; 105:4820. [PubMed: 15728130]
21. Zhe X, Cher ML, Bonfil RD. American Journal of Cancer Research. 2011; 1:740. [PubMed: 22016824]
22. Sieuwerts AM, Kraan J, Bolt J, Spoel Pvd, Elstrodt F, Schutte M, Martens JWM, Gratama J-W, Sleijfer S, Foekens JA. Journal of the National Cancer Institute. 2009; 101:61. [PubMed: 19116383]
23. Xu H, Aguilar ZP, Yang L, Kuang M, Duan H, Xiong Y, Wei H, Wang A. Biomaterials. 2011; 32:9758. [PubMed: 21920599]
24. Olmos D, Arkenau H-T, Ang JE, Ledaki I, Attard G, Carden CP, Reid AHM, A'Hern R, Fong PC, Oomen NB, Molife R, Dearnaley D, Parker C, Terstappen LWMM, Bono JSd. Annals of Oncology. 2009; 20:27.
25. Cohen SJ, Punt CJA, Iannotti N, Saidman BH, Sabbath KD, Gabrail NY, Picus J, Morse MA, Mitchell E, Miller MC, Doyle GV, Tissing H, Terstappen LWMM, Meropol NJ. Annals of Oncology. 2009; 20:1223. [PubMed: 19282466]
26. Wu C-H, Huang Y-Y, Chen P, Hoshino K, Liu H, Frenkel EP, Zhang JXJ, Sokolov KV. ACS Nano. 2013; 7:8816. [PubMed: 24016305]
27. McGuckin C, Jurga M, Ali H, Strbad M, Forraz N. Nature Protocols. 2008; 3:1046. [PubMed: 18536651]
28. Tiwari A, Punshon G, Kidane A, Hamilton G, Seifalian AM. Cell Biology and Toxicology. 2003; 19:265. [PubMed: 14703114]
29. Chalmers JJ, Zborowski M. Analytical Chemistry. 2011; 83:8050. [PubMed: 21812408]
30. Plouffe BD, Murthy SK, Lewis LH. Reports on Progress in Physics. 2015; 78:016601. [PubMed: 25471081]
31. Yang L, Lang JC, Balasubramanian P, Jatana KR, Schuller D, Agrawal A, Zborowski M, Chalmers JJ. Biotechnology and Bioengineering. 2009; 102:521. [PubMed: 18726961]
32. Salvati A, Pitek AS, Monolopli MP, Prapainop K, Bombelli FB, Hristov DR, Kelly PM, Aberg C, Mahon E, Dawson KA. Nature Nanotechnology. 2013; 8:137.
33. Laurent S, Saei AA, Behzadi S, Panahifar A, Mahmoudi M. Expert Opinion on Drug Delivery. 2014; 11:1449. [PubMed: 24870351]
34. Rana D, Matsuura T. Chemical Reviews. 2010; 110:2448. [PubMed: 20095575]
35. Mirshafiee V, Mahmoudi M, Lou K, Cheng J, Kraft ML. Chemical Communications. 2013; 49:2557. [PubMed: 23423192]
36. Chalmers JJ, Xiong Y, Jin X, Shao M, Tong X, Farag S, Zborowski M. Biotechnology and Bioengineering. 2010; 105:1078. [PubMed: 20014141]
37. Wu J, Gao L, Gao D. ACS Applied Materials & Interfaces. 2012; 4:3041. [PubMed: 22568650]
38. Li J, Zhou Y, Li M, Xia N, Huang Q, Do H, Liu Y-N, Zhou F. Journal of Nanoscience and Nanotechnology. 2011; 11:10187. [PubMed: 22413363]
39. Barrow M, Taylor A, Nieves DJ, Bogart LK, Mandal P, Collins CM, Moore LR, Chalmers JJ, Levy R, Williams SR, Murray P, Rosseinsky M, Adams DJ. Biomaterials Science. 2015; 3:608. [PubMed: 26222421]
40. Gilbertson RJ. The Lancet Oncology. 2004; 5:209. [PubMed: 15050952]
41. Li Y, Lin R, Wang L, Huang J, Wu H, Cheng G, Zhou Z, MacDonald T, Yang L, Mao H. Journal of Materials Chemistry B. 2015; 3:3591.
42. Huang J, Wang L, Zhong X, Li Y, Yang L, Mao H. Journal of Materials Chemistry B. 2014; 2:5344.
43. Byrd TF, Horwitz MA. The Journal of Clinical Investigation. 1993; 91:969. [PubMed: 8450071]
44. Ganong, WF. Review of Medical Physiology. McGraw-Hill; 2003.
45. Nai A, Lidonnici MR, Rausa M, Mandelli G, Pagani A, Silvestri L, Ferrari G, Camaschella C. Blood. 2015; 125:1170. [PubMed: 25499454]

46. Szaniszlo P, Wang N, Sinha M, Reece LM, Van Hook JW, Luxon BA, Leary JF. Cytometry A. 2004; 59:191. [PubMed: 15170598]
47. Altelaar AFM, Heck AJR. Current Opinion in Chemical Biology. 2012; 16:206. [PubMed: 22226769]
48. Nel AE, Madler L, Velegol D, Xia T, Hoek EMV, Somasundaran P, Klaessig F, Castranova V, Thompson M. Nature Materials. 2009; 8:543. [PubMed: 19525947]
49. Nie S. Nanomedicine. 2010; 5:523. [PubMed: 20528447]
50. Sanhai WR, Sakamoto JH, Canady R, Ferrari M. Nature Nanotechnology. 2008; 3:242.
51. Weissleder R, Nahrendorf M, Pittet M. Nature Materials. 2014; 13:125. [PubMed: 24452356]
52. Allard WJ, Matera J, Miller MC, Repollet M, Connelly MC, Rao C, Tibbe AG, Uhr JW, Terstappen LWMM. Clinical Cancer Research. 2004; 10:6897. [PubMed: 15501967]
53. Nagrath S, Sequist LV, Maheswaran S, Bell DW, Irimia D, Ulkus L, Smith MR, Kwak EL, Digumarthy S, Muzikansky A, Ryan P, Balis UJ, Tompkins RG, Haber DA, Toner M. Nature. 2007; 450:1235. [PubMed: 18097410]

Highlights

- Anti-fouling IONPs retain targeting capability upon the exposure to medium protein
- IONPs are more sensitive and specific to targeted cells with anti-fouling coating.
- Anti-fouling IONPs have higher efficiency in targeted cell separation than Dynabeads.

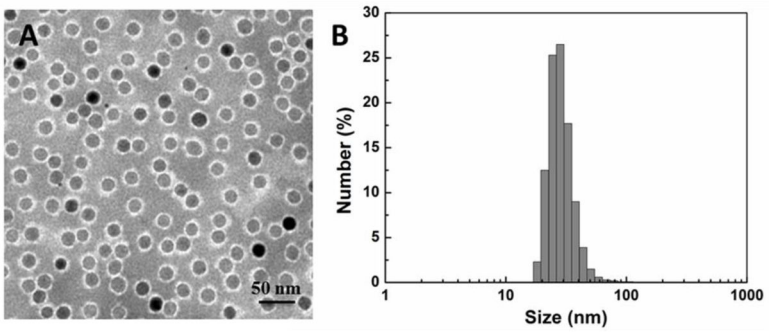

Figure 1.

(A) TEM images with negative stain showed a polymer coating (bright annular layer surrounding the particles) of IONPs with 20 nm core. (B) Dynamic light scattering (DLS) data showed the hydrodynamic sizes (in diameter) of PEG-*b*-AGE polymer coated IONPs with 20 nm core.

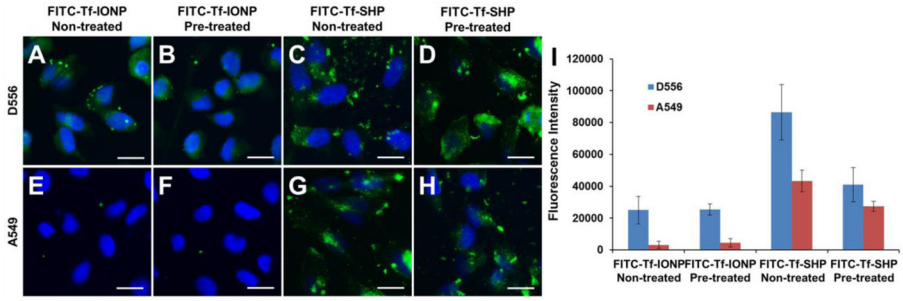

Figure 2.

Fluorescent images of D556 medulloblastoma cells incubated with (A) FITC-Tf-IONP with no FBS pre-treatment, (B) FBS pre-treated FITC-Tf-IONP, (C) FITC-Tf-SHP with no FBS treatment, and (D) FBS pre-treated FITC-Tf-SHP; A549 lung cancer cells take up (E) FITC-Tf-IONP with no FBS pre-treatment, (F) FBS pre-treated FITC-Tf-IONP, (G) FITC-Tf-SHP with no FBS treatment, and (H) FBS pre-treated FITC-Tf-SHP. (I) Fluorescent signal intensities of FITC from FBS pre-treated or no FBS treated IONPs taken up by D556 medulloblastoma or A549 lung cancer cells. Scale bar 20 μm.

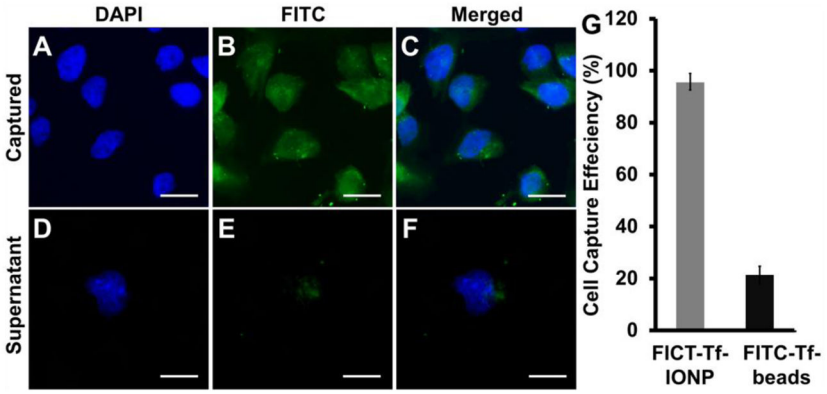

Figure 3.

Fluorescent images of D556 medulloblastoma cells captured by FITC-Tf-IONP: (A) DAPI, (B) FITC, and (C) merged; fluorescent images of D556 medulloblastoma cells left in supernatant: (D) DAPI, (E) FITC, and (F) merged. (G) Efficiency of D556 cells capture using FITC-Tf-IONP and FITC-Tf- beads. Scale bar 20 μm.

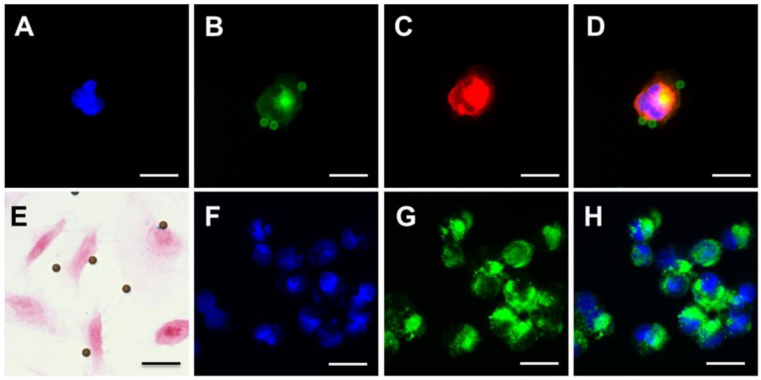

Figure 4.

Fluorescent images of Dil pre-stained D556 medulloblastoma cell isolated by FITC-Tf-beads: (A) DAPI, (B) FITC, (C) Dil, and (D) merged image of DAPI, FITC and Dil. (E) Prussian blue stained image of D556 medulloblastoma cells treated with FITC-Tf-beads. Fluorescent images of D556 medulloblastoma cells isolated by FITC-Tf-IONP: (F) DAPI, (G) FITC, (H) merged. Scale bar 20 μm.

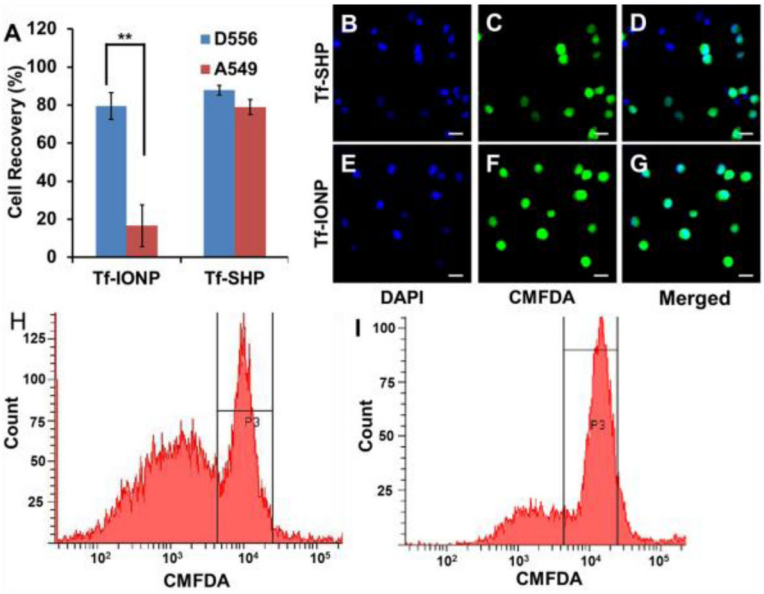

Figure 5.

(A) D556 medulloblastoma cells and A549 lung cancer cells capture rate using Tf-IONP or Tf-SHP (** $p<0.01$). Fluorescent images of cells captured by the Tf-SHP: (B) DAPI, (C) CMFDA, and (D) merged; and by Tf-IONP: (E) DAPI, (F) CMFDA, (G) merged. Scale bar 20 μm. Flow cytometry count/signal intensity of captured cells from mixtures of pre-stained D556 cells with equal amount of A549 cells by (H) Tf-SHP and (I) Tf-IONP.

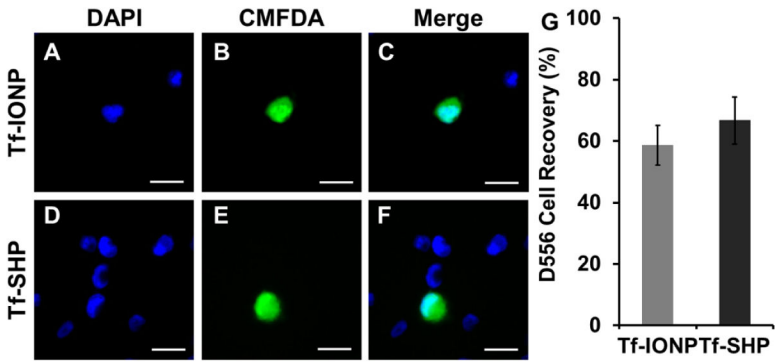

Figure 6.

Fluorescent images of CMFDA pre-stained D556 medulloblastoma cells (green) isolated by Tf-IONP from a mixture of D556 medulloblastoma cells with 1000-fold A549 lung cancer cells: (A) DAPI, (B) CMFDA, (C) merged; and by Tf-SHP: (D) DAPI, (E) CMFDA, (F) merged. Scale bar 20 μm. (G): Quantification of captured D556 medulloblastoma cells from a mixture of pre-stained D556 cells with 1000-fold A549 lung cancer cells.

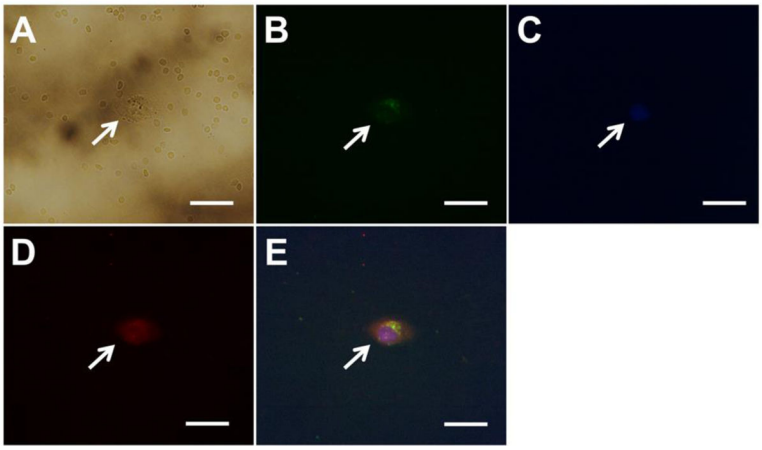

Figure 7.

Images of one D556 medulloblastoma cell separated from one mL of whole blood using anti-biofouling FITC-Tf-IONPs: (A) bright field, (B) FITC, (C) DAPI, (D) TRITC, and (E) merged fluorescent image. Scale bar 20 μm.

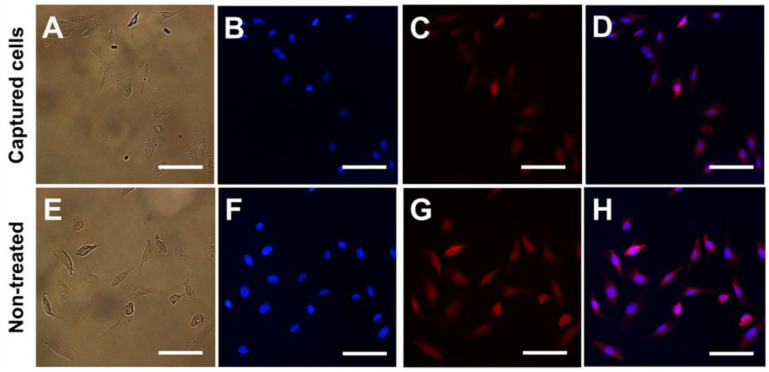

Figure 8.

Images of proliferated D556 medulloblastoma cells separated from blood by FITC-Tf-IONPs: (A) bright field, (B) DAPI, (C) TRITC, and (D) merged fluorescent images. Images of non-treated D556 medulloblastoma cells n: (E) bright field, (F) DAPI, (G) TRITC, and (H) merged fluorescent images. Scale bar 100 μm.

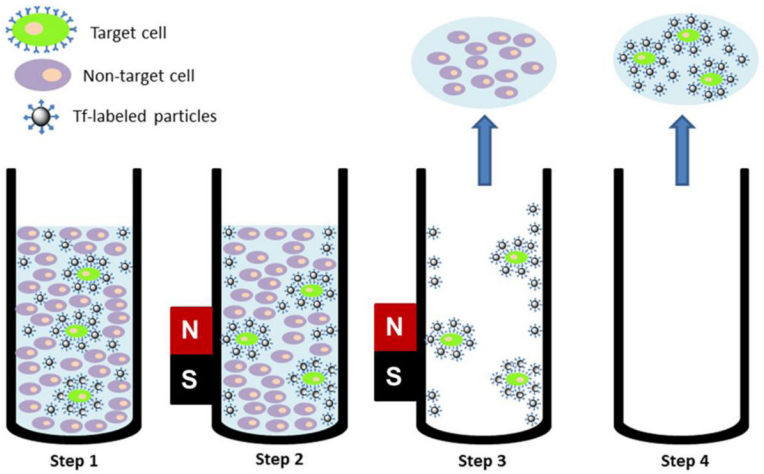

Scheme 1.

Diagram depicting the procedure of capturing targeted cells. Step 1: Tf-labeled particles bound to targeted cells which were spiked into medium containing a larger amount of non-targeted cells. Step 2: Magnetic separation. Step 3: Removal of supernatant as well as non-target cells. Step 4: Re-suspending and obtaining target cells.

Table 1

Hydrodynamic diameters and zeta potentials of nanoparticles with different surface modifications*

Properties	PEG-*b*-AGE coated IONPs	Tf-IONPs	SHP	Tf-SHP
D_H (nm)	30.46±1.65	36.59±2.14	24.73±0.61	30.80±2.90
ζ potential (mV)	15.57±0.60	−26.07±3.71	−43.2±0.953	−28.2±1.65

*All nanoparticles have the same core size of 20 nm in diameter.